

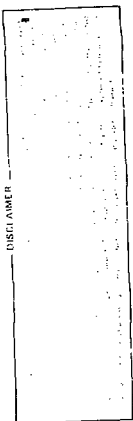
Numerical Treatment of the Axial Singularity
in a Flux-Coordinate System

Gioietta Kuo-Petravic

Plasma Physics Laboratory, Princeton University

P.O. Box 451

Princeton, New Jersey 08544



In the realistic simulation of physical systems whether in 2-D or 3-D there arise often situations where the fluid flow has a preferred direction. An example of this is a magnetically confined plasma where the flow is predominantly along the magnetic field lines. To avoid a large numerical diffusion and hence inaccuracy, it is often necessary to adopt a flux coordinate system with coordinates following closely the contours given naturally by the physics of the problem, an example for this is shown in fig. 1. In this system radial motion is measured by the flux function $\psi = \oint \vec{B} \cdot d\vec{A}$, where \vec{B} is the magnetic field and \vec{A} an enclosed area whose boundary is traced out by the intersections of a magnetic field line with a poloidal plane. The angular variable θ_0 is measured from the axis which is at the center of the set of nested ψ surfaces. This point at $\psi = 0$ corresponds to multivalued values of θ_0 and this causes most general numerical methods to break down. However we shall show here that it is possible and efficient in computer time to overlay the ψ, θ_0 mesh with a rectangular x, y mesh near the origin. With this transformation the peculiarities of the singular point disappear and ordinary numerical techniques can be carried through.

We shall use as an example a problem we have encountered in our

simulation of a plasma in an asymmetric torus [1,2]. Here the fact that a flux surface is also an equipotential surface gives additional incentive for the use of flux coordinates. The equations for the drift motion of ions in a magnetic field can be cast in a very simple Hamiltonian form which can be easily integrated [2] if the flux coordinates θ_o, ψ, χ are used. Here ψ is the toroidal flux, θ_o a poloidal angle measured from the magnetic axis and χ is a coordinate along the magnetic field line. Since χ does not enter into our essentially 2 dimensional problem we shall henceforth restrict ourselves to θ_o, ψ only.

The drift equations are:

$$\frac{d\theta_o}{dt} = -A \frac{\partial B}{\partial \psi} - \frac{\partial \Phi}{\partial \psi}$$

$$\frac{d\psi}{dt} = A \frac{\partial B}{\partial \theta_o} \tag{1}$$

where B is the magnetic field and

$$A = \mu + \rho_{\parallel}^2 B, \text{ where } \mu = \text{the magnetic moment,} \\ \rho_{\parallel} = \text{the parallel Larmor radius, and}$$

$\Phi(\psi) = \text{electric potential .}$

When these equations are integrated very close to $\psi = 0$, the singularity at the axis manifests itself most commonly as the unphysical condition $\psi < 0$ when an integration scheme like the 4th order Runge-Kutta is used. Although the probability of this occurring is in general of the order of the ratio of a few times $\pi \nabla \psi^2$ to the total flux area, where $\nabla \psi$ is the change in ψ in one time step, (in our case this ratio is around 10^{-4}), it is very inconvenient

especially when particles have long confinement times and the runs abort before data collection is complete.

In our method we transform to an x,y system using circularized flux surfaces:

$$\begin{aligned}x &= (2\psi)^{1/2} \cos \theta_o \\y &= (2\psi)^{1/2} \sin \theta_o\end{aligned}\quad (II)$$

We then advance the x,y coordinates in time instead of the θ_o, ψ coordinates using the equations:

$$\begin{aligned}\frac{dx}{dt} &= \frac{1}{(2\psi)^{1/2}} \cos \theta_o \left(\frac{d\psi}{dt}\right) - (2\psi)^{1/2} \sin \theta_o \left(\frac{d\theta_o}{dt}\right) \\ \frac{dy}{dt} &= \frac{1}{(2\psi)^{1/2}} \sin \theta_o \left(\frac{d\psi}{dt}\right) + (2\psi)^{1/2} \cos \theta_o \left(\frac{d\theta_o}{dt}\right)\end{aligned}\quad (III)$$

Since for any given x,y the corresponding θ_o, ψ can be calculated everywhere using the equations (II), we are able to derive the values of $d\psi/dt$ and $d\theta_o/dt$ from equations (I) once the gradients of B in the θ_o, ψ coordinate system are known. Therefore:

$$\begin{aligned}\frac{dx}{dt} &= \frac{A \cos \theta_o}{(2\psi)^{1/2}} \frac{\partial B}{\partial \theta_o} + (2\psi)^{1/2} \sin \theta_o \left[\frac{\partial \Phi}{\partial \psi} + A \frac{\partial B}{\partial \psi} \right] \\ \frac{dy}{dt} &= \frac{A \sin \theta_o}{(2\psi)^{1/2}} \frac{\partial B}{\partial \theta_o} + (2\psi)^{1/2} \cos \theta_o \left[\frac{\partial \Phi}{\partial \psi} + A \frac{\partial B}{\partial \psi} \right]\end{aligned}\quad (IV)$$

The magnetic field near the axis can be expanded in the form:

$$B = \sum_{n,m} \psi^{|m|/2} (a + b\psi + c\psi^2 \dots) \cos(\omega\chi - m\theta_0) \quad (V)$$

where n = toroidal mode number
 m = poloidal mode number
 $\omega = (n - m_1)/g$
 g = total poloidal current
 i = rotational transform

from which

$$\begin{aligned} \frac{\partial B}{\partial \theta_0} &= \sum_{n,m} m \psi^{|m|/2} (a + b\psi + c\psi^2 + d\psi^3) \sin(\omega\chi - m\theta_0) \\ \frac{\partial B}{\partial \psi} &= \sum_{n,m} \left[\frac{|m|}{2} \psi^{\left(\frac{|m|}{2} - 1\right)} (a + b\psi + c\psi^2 + d\psi^3) \cos(\omega\chi - m\theta_0) \right. \\ &\quad + \psi^{|m|/2} (b + 2c\psi + 3d\psi^2) \cos(\omega\chi - m\theta_0) \\ &\quad \left. - \psi^{|m|/2} (a + b\psi + c\psi^2 + d\psi^3) \sin(\omega\chi - m\theta_0) \left[\frac{m_1}{g} \chi \right] \right] \quad (VI) \end{aligned}$$

For $|m| = 1$ the first term of the second equation in (VI) tends to infinity as ψ goes to 0. This is of course the reason why eqns (I) are not useful near the origin. However when (VI) is incorporated into the Cartesian formulation in (IV) the multiplying factor $\psi^{1/2}$ removes the singularity in the first term of $\frac{\partial B}{\partial \psi}$. This must hold for any B which is physical as Eq. (IV) is valid so long as B is analytic near $\psi = 0$.

We have implemented the algorithm outlined above and Fig. (2) shows the projected trajectory in θ_0, ψ plane of a particle whose path straddles the boundary at $\psi = \psi_c$. For $\psi < \psi_c$ the particle position is advanced in x, y space while for the region $\psi_c < \psi < \psi_a$ the computation is entirely in θ_0, ψ space. Here $\psi_c = 10^{-4}$ and $\psi_a = 1$. The choice of ψ_c depends mostly on the maximum $\Delta\psi$ the particle makes per time step in the region around $\psi = 0$. To prevent the

particle from crossing the axial region in one step starting from $\psi > \psi_c$, it is desirable to make $\psi_c / \Delta\psi \gtrsim 10$.

Major alteration to the computer program is only required in the subroutine supplying the RHS of (IV) to the Runge-Kutta control subroutine. In order to retain as much as possible the vectorization benefits of the CRAY-I compiler, we make the same array store either (θ_o, ψ) or (x, y) depending on the value 0 or 1 of a switch. This switch is used to direct the flow to either the (θ_o, ψ) or the (x, y) blocks of code. Testing on ψ to find out if the particle has just entered or left the x, y computational region given by $\psi < \psi_c$ is performed once per time step in the main program.

An alternative solution when eqns (IV) are only used when $\psi_c \ll 1$ is to drop all higher terms in the polynomial for B, (V), keeping only the constant term. This was found to reduce the computer time required for one timestep by 20%.

Acknowledgment

This work was supported by United States Department of Energy Contract No. DE-ACC2-76-CH03073.

I wish to thank R.C. Grimm and R. B. White for their helpful discussions.

References

- [1] G. Kuo-Petravic, A. H. Boozer, J. Rome, and R. Fowler to appear in J. Compt. Phys. (1982).
- [2] A. H. Boozer and G. Kuo-Petravic, Phys. Fluids 24, 831 (1981).
- [3] A. H. Boozer, Phys. Fluids (1982).

Figure Captions

Fig. 1. Schematic diagram of a 2-D flux coordinate system θ, ψ .

Fig. 2. Projections of a trajectory of a particle in an asymmetric toroidal plasma device. Points inside the circle $\psi = \psi_c$ are calculated in (x, y) system and points outside in (θ, ψ) system.

82 T 0114

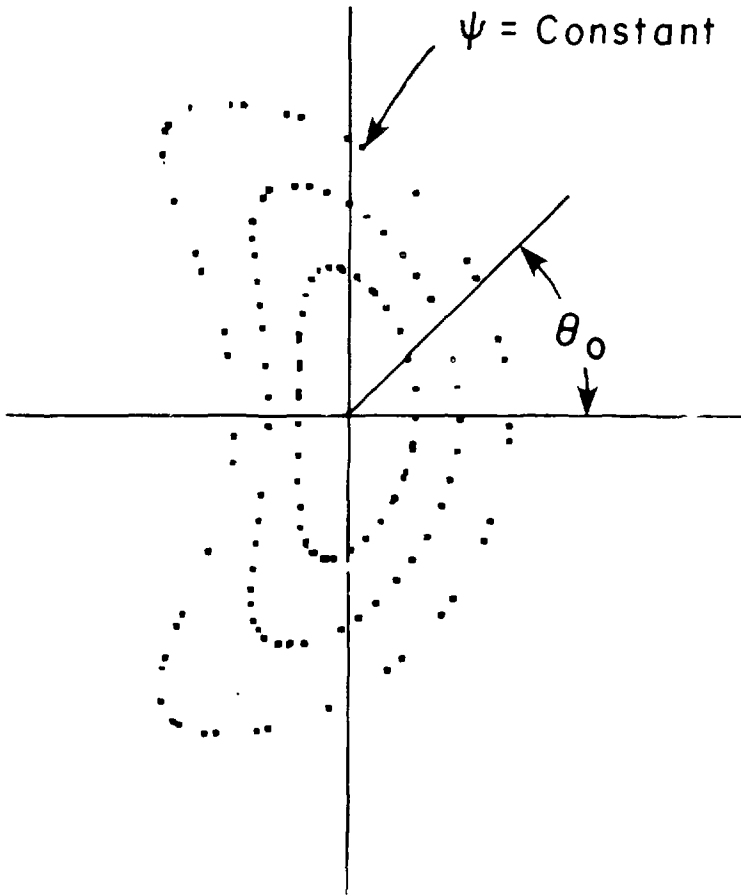


Fig. 1

82 T 0113

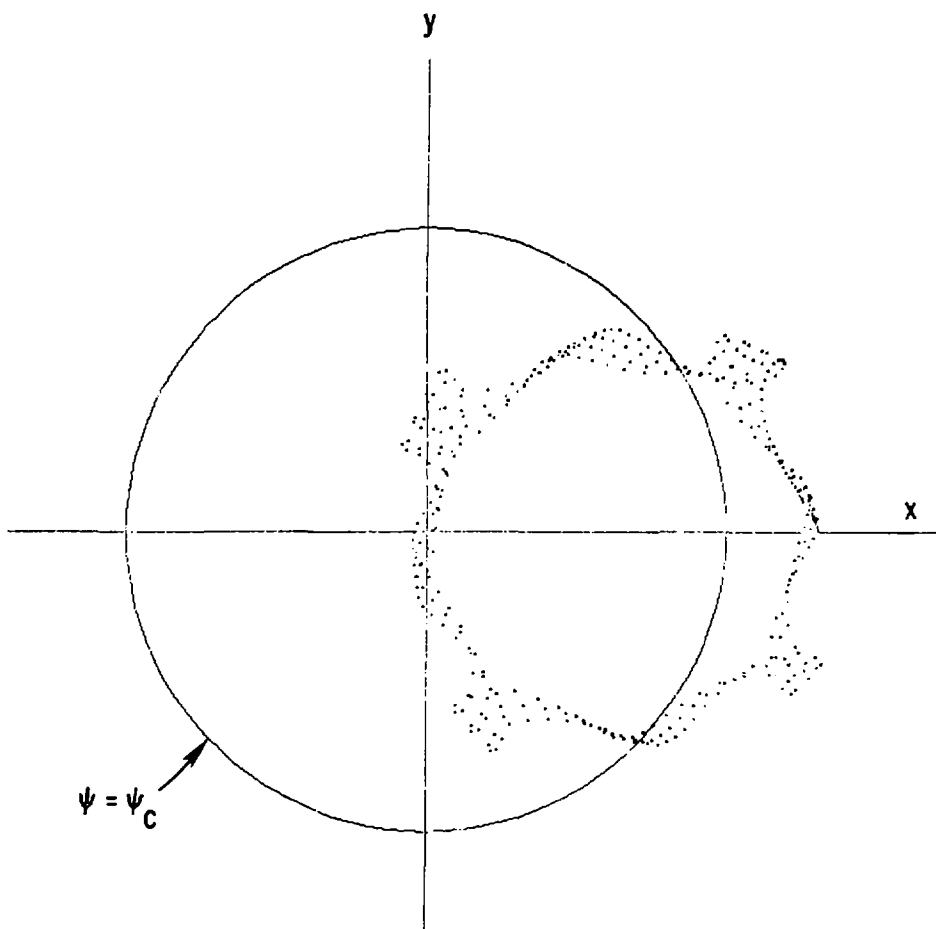


Fig. 2